Colorado School of Mines
Physics Department
1523 Illinois Street
Golden, Colorado 80402
January 31, 2006

Ken Zweibel
Technical Monitor
National Renewable Energy Laboratory
1617 Cole Boulevard
Golden, Colorado 80401-3393

Subject: CSM Extension of ADJ-2-30630-05, Studies of Basic Electronic Properties of CdTe-based Solar Cells.

Principal Investigators and key personnel: Dr. Joseph D. Beach Jr.
Dr. Victor Kaydanov
Dr. Timothy R. Ohno
Dr. Fred H. Seymour

Dear Ken,

During the first quarter of the subcontract extension (1 November 2005 - 31 January 2006) the following work was performed.

Task 1. Study of Deep Electronic States controlling V_{OC}.

The goal of this deep electronic states (DES) study is to detect, characterize, and identify DES that may be either limiting or enhancing V_{OC} in order to help cell growers modify their processes to improve their devices. A J-V-T, QE, and impedance characterization analysis was performed on cells received from X. Wu that were processed without intentionally added Cu and with three $CdCl_2$ treatments. This compliments a set of previously analyzed cells with added Cu and the same three $CdCl_2$ treatments. This is part of an ongoing collaborative study with Wu. Further analyses are expected with variable Cu and O_2 applied in the processing.

The room temperature J-V measurements taken at CSM for the six cells with and without Cu and the three $CdCl_2$ treatments are shown in table 1. The Cu treatment had more impact on cell performance. This contrasts with cells previously analyzed[1] from D. Albin and B. McCandless where the $CdCl_2$ treatment had the greater impact on performance. In Wu's cells the short circuit dynamic series resistance ("shunt resistance") increased with the Cu treatment and this has not been typically observed. The 2nd level metrics V_{OC}, J_{SC} and FF were improved by the Cu treatment with one exception. With the optimal $CdCl_2$ treatment (15' @ 405°C) the no Cu cell had a better J_{SC}. This has been observed in the cells from Albin and McCandless.

Table 1. CSM J-V results on cells studied from X. Wu.

Cell	Treat	Eff %	V_{OC} mV	J_{SC} mA cm^{-2}	FF %	R_{SC} Ω cm^2	R_{OC} Ω cm^2
W1226-2	yes Cu, 15' $CdCl_2$ @405C	14.06	826	23.7	71.8	1361	2.8
W1226-8	no Cu, 15' $CdCl_2$ @405C	7.20	657	24.6	44.5	191	15.4
W1226-4	yes Cu, no $CdCl_2$	10.44	754	20.9	66.3	491	3.3
W1226-7	no Cu, no $CdCl_2$	8.47	734	18.9	61.1	369	8.0
W1226-3	yes Cu, 15' $CdCl_2$ @425C	10.88	801	23.5	57.8	261	4.9
W1226-9	no Cu, 15' $CdCl_2$ @405C	2.24	463	14.8	32.7	83	28.3

QE data showed higher near band edge (~840nm) collection as well as higher blue (~450nm) collection for the high temperature $CdCl_2$ treated cells (15' @425C). This indicates increased CdS/CdTe intermixing and a thinner effective window layer. For the non-$CdCl_2$ treated cells, the QE data showed the least CdS/CdTe intermixing as well as the least collection for wavelengths around 550 nm, which is absorbed in the CdTe near the CdS/CdTe interface.

J-V-T data shows increasing V_{OC} with decreasing temperature. A possible explanation for this effect is that V_{OC} limiting deep level electronic states are freezing out as the temperature decreases. This effect is less pronounced on the two cells that had the $CdCl_2$ treatment with no Cu. This is consistent with previous observations[1] on cells from Albin, but less so on cells from McCandless.

The J-V-T data for J_{SC} shows an abrupt decrease in current collection starting at –120^{o}C for the $CdCl_2$ treated cells. A possible explanation for this is that V_{Cd} and related complex defects with E_a~0.15eV are the dominant dopants in the $CdCl_2$ treated cells and they start freezing out at these temperatures. This is consistent with observations on cells from Albin and McCandless.

A total of twenty DES were detected and these were grouped into seven distinct signatures between the six cells. The Arrhenius plot for these results are shown in Fig. 1. The H1, H2, H3, and H3B signatures at the top of the graph were detected with admittance spectroscopy[2] (AS) analysis. The E2, E3, and H5 signatures at the bottom of the graph were detected with capacitance transients[3] (CTr) analysis. These defect signatures are consistent with those detected in cells from Albin and McCandless. A complete listing of the detected defects is in Table 2.

The H1 signature which has been identified as V_{Cd}^{-} and related complexes[2] had measurable $dC_p / d\ln(\omega)$ peaks in the cells processed with Cu. With the other cells, while there were no peaks, there were indications that the H1 DES is present with a range of E_a values. This could be a result of distortions from band bending and the AS measurement technique or it could be an actual band of DES energy levels. Based on the J-V-T data it is possible that this H1 defect is the dopant that enables superior current collection in the $CdCl_2$ treated cells.

H2, which has been previously identified as Cu_{Cd}^{-} is only detected in the Cu treated cells. The indicated concentration of Cu_{Cd}^{-} based on C_t^0 is the largest without the $CdCl_2$ treatment. There are not yet experimental indications for what role, if any, this defect might have in the superior performance of the Cu treated cells.

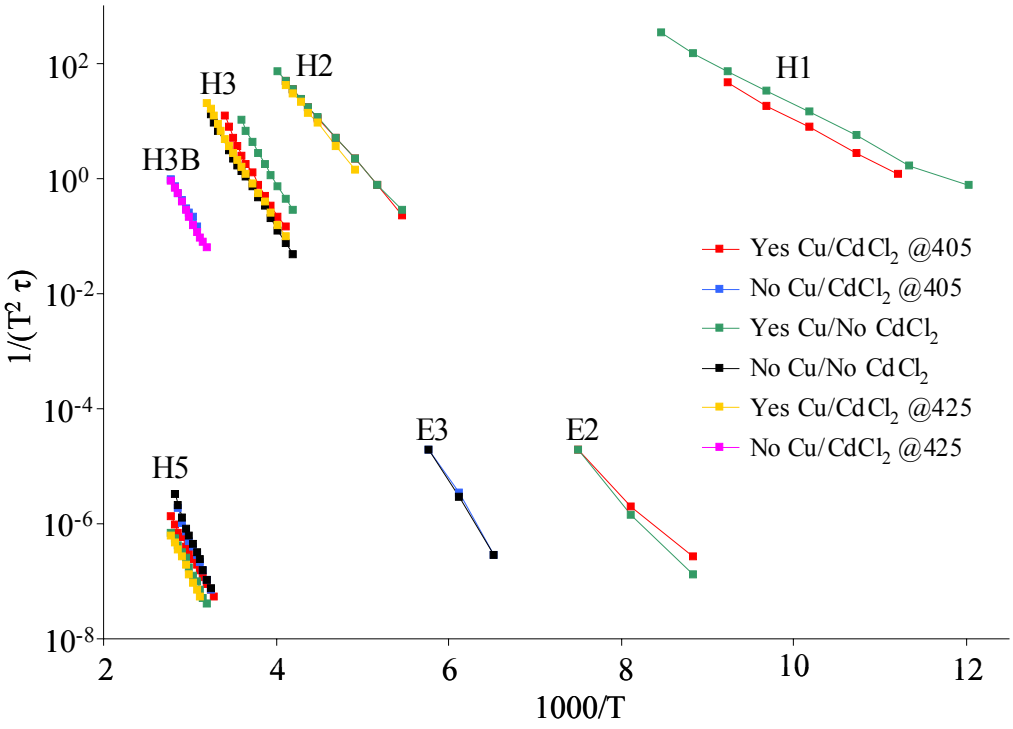

FIG. 1 Arrhenius plot of deep electronic states detected on cells produced by Wu with admittance spectroscopy (top) and capacitance transients (bottom).

The H5 defect is of interest because it has a very strong signature in the cells that have both the Cu and $CdCl_2$ treatments. The magnitude of C_t^0, the capacitance attributed to the defect, is an order of magnitude larger than that from any other detected defect, indicating that it has a high concentration. We have also detected H5 with similar magnitudes in the Cu and $CdCl_2$ treated cells from Albin and McCandless.

H5 is close to mid-gap and could act as a SRH recombination center. However, its apparent capture cross section is small. It is possible that it is located in the CdS/CdTe intermix zone. We suspect this because the signature is strongest with a forward bias pulse, which shrinks the depletion region to the vicinity of the intermix zone. We have not yet identified H5 and it is not yet clear what role this defect might have in the cell's performance.

The minority carrier CTr defect E2 occurs with Cu processing and E3 occurs without Cu. The H3 and H3B occur mostly without the Cu treatment. This is consistent with

observations on cells from Albin and McCandless and their impact on cell performance is not known.

Table 2. Defects detects with admittance spectroscopy (H1, H2, H3, H3B) and with capacitance transients (E2, E3, H5) on cells produced by Wu.

DES	Cu/$CdCl_2$	E_a (eV)	σ_a (cm^2)	C_t^0 (nF cm^{-2})	Temp range (K)
H1	Yes/405°C	0.16 ±0.01	$5X10^{-13}$	NA	89-108
	Yes/No	0.15 ±0.01	$3X10^{-13}$	1.0	83-118
H2	Yes/405°C	0.34 ±0.01	$2X10^{-13}$	0.4	183-243
	Yes/No	0.33 ±0.01	$1X10^{-13}$	0.7	183-248
	Yes/425°C	0.36 ±0.01	$6X10^{-13}$	0.2	203-243
H3	Yes/405°C	0.54 ±0.03	$7X10^{-12}$	0.6	243-293
	Yes/No	0.52 ±0.02	$9X10^{-12}$	1.0	238-277
	No/No	0.49 ±0.01	$5X10^{-13}$	4.0	238-308
	Yes/425°C	0.50 ±0.01	$8X10^{-13}$	1.0	243-312
H3B	No/405°C	0.54 ±0.05	$1X10^{-14}$	2.0	324-358
	No/425°C	0.57 ±0.02	$4X10^{-14}$	8.0	312-358
E2	Yes/405°C	0.28 ±0.32	$2X10^{-16}$	-0.3	113-133
	Yes/No	0.32 ±0.30	$1X10^{-14}$	-0.8	113-133
E3	No/405°C	0.48 ±0.45	$7X10^{-13}$	-0.1	153-173
	No/No	0.48 ±0.17	$6X10^{-13}$	-0.6	153-173
H5	Yes/405°C	0.55 ±0.01	$2X10^{-20}$	40.0	304-358
	No/405°C	0.71 ±0.05	$1X10^{-17}$	6.0	308-348
	Yes/No	0.60 ±0.02	$9X10^{-20}$	10.0	312-358
	No/No	0.76 ±0.04	$8X10^{-17}$	6.0	308-353
	Yes/425°C	0.63 ±0.02	$2X10^{-19}$	60.0	320-358

Task 2. Test different cell growth approaches that can lead to higher V_{OC}.

The goal at this time is to better understand the sensitivity of cell performance to different processing parameters used with the gas jet cell growth system[4] at CSM. At this stage with TEC15 glass single layer TCO we can reliably produce >8% cells with V_{OC} > 650 mV. A study of the performance impact of the post-deposition processing Cu/ZnTe anneal temperature was undertaken and is described below.

A 1.5x1.5x1/8 inch TEC-15 glass plate was used as a substrate. Approximately 200nm of CBD CdS was deposited followed by 3-5 microns gas jet CdTe (the gasjet system yields a thicker CdTe layer at the center of the plate than at the edges). A $CdCl_2$ anneal was performed prior to the Cu/ZnTe back contact anneal.

The Cu/ZnTe rapid thermal anneal (RTA) back contact treatment consists of a bromine methanol etch preparation followed by evaporating 10Å of Cu and 500 Å of ZnTe onto the back surface. The cell is put in a carbon boat that is placed in a bell jar, then it is evacuated and back filled with nitrogen. The boat is heated for 3-5 minutes to drive the Cu into the cell. When the boat temperature reaches the set temperature, the heating element is turned off. Following this, circular gold dots of 0.79cm^2 in a hexagonal pattern are evaporated onto the plate to finish the device. Approximately 50 cells are produced from a single plate.

In this study, following the gold contact deposition, RTA temperatures were applied in succession ranging from 150 ^{o}C to 400 ^{o}C in increments of 50 ^{o}C. J-V results averaged from the top 21 cells out of 26 tested are tabulated in table 3. The standard deviations are listed to help gage the cell to cell non-uniformity within a single plate. The 300 ^{o}C RTA demonstrated the best performance as well as the least non-uniformity. This is now the default RTA temperature for our process.

It is evident that the back contact anneal temperature significantly impacts V_{OC} as well as R_{SC}, the short circuit dynamic resistance or "shunt" resistance.

Table 3. CSM J-V RTA range of temperature results which includes the average value and standard deviation from top 21 cells following each successive higher temperature anneal.

RTA ^{o}C	Eff %	V_{OC} mV	J_{SC} mA cm^{-2}	FF %	R_{SC} Ω cm^2	R_{OC} Ω cm^2
None	4.8 ±1.3	500 ±40	20.8 ±3.2	46 ±3	122 ±92	8.5 ±1.4
150	4.8 ±1.7	546 ±33	18.5 ±4.4	47 ±4	148 ±112	9.1 ±1.5
200	5.4 ±1.8	624 ±16	18.7 ±4.3	45 ±5	164 ±124	9.2 ±2.1
250	6.4 ±1.7	672 ±18	20.9 ±2.9	44 ±7	195 ±141	8.7 ±2.1
300	8.2 ±0.6	660 ±13	23.1 ±0.4	53 ±3	530 ±150	9.9 ±2.3
350	6.3 ±1.6	609 ±100	22.7 ±0.7	45 ±7	316 ±106	22.8 ±12.2
400	3.9 ±1.4	570 ±89	21.4 ±1.2	32 ±8	197 ±129	99.2 ±82.4

A J-V graph of for a single cell over the range of RTA temperatures is shown in Fig. 2. For the "under-annealed" 250 ^{o}C cell a voltage dependent current collection is evident. This could indicate a weak electric field or lateral non-uniformity with weak diodes. For the "over-annealed" 350 ^{o}C cell the roll-under is similar to that of severely degraded cells.

A study on the effects of oxygen concentration during deposition and the $CdCl_2$ anneal is underway. Preliminary indications are that additional oxygen (50% O_2, 50% N_2) during the $CdCl_2$ anneal will allow >10% cells with V_{OC} > 700 mV.

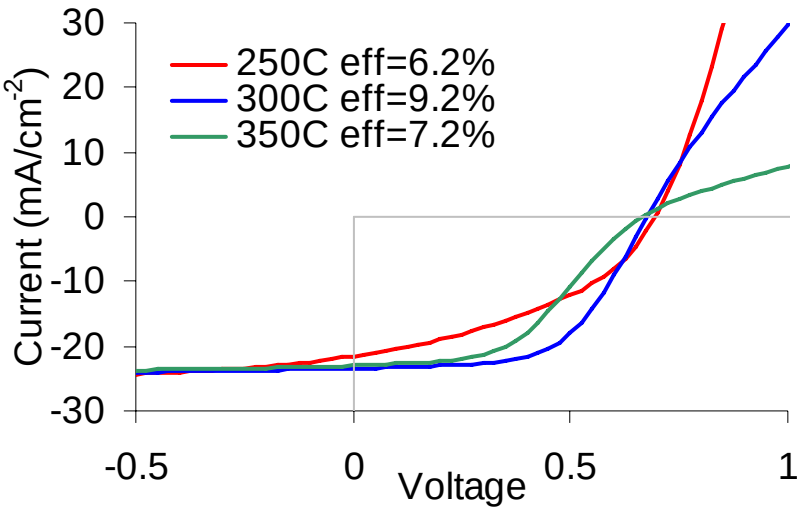

FIG 2. J-V curves for RTA temperatures bracketing the optimum efficiency.

Sincerely,

Fred H. Seymour

.

References

[1]F. H. Seymour, Ph.D. thesis, Colorado School of Mines, October 20, 2005.

[2]F. H. Seymour, V. Kaydanov, T. R. Ohno, D. Albin, J. Appl. Phys. 87, 153507, Oct. 2005.

[3]F. H. Seymour, V. Kaydanov, T. R. Ohno, Proceedings from the 31st IEEE Photovoltaics Specialists Conference, Orlando, Florida, Jan. 3-7, 2005, pp. 275-278.

[4]J. M. Kestner, Ph.D. thesis, Colorado School of Mines, April 2003.